ISSN 1063-7826, Semiconductors, 2009, Vol. 43, No. 13, pp. 1628–1634. © Pleiades Publishing, Ltd., 2009.
Original Russian Text © N.K. Morozova, N.D. Danilevich, V.M. Semenov, V.G. Galstyan, V.I. Oleshko, S.S. Vil'chinskaya, V.M. Lisitsyn, 2009, published in Izvestiya vysshikh uchebnykh zavedenii. Elektronika, 2009, Vol. 43, No. 13.

BASIC
RESEARCH

Some Specific Features of Edge Luminescence of CdS(O) in the Context of the Band's Anticrossing Theory

N. K. Morozova[a], N. D. Danilevich[a], V. M. Semenov[a], V. G. Galstyan[b], V. I. Oleshko[c], S. S. Vil'chinskaya[c], and V. M. Lisitsyn[c]

[a]*Moscow Power Engineering Institute (Technical University), Moscow, 111250 Russia*
e-mail: morozovank@mail.ru
[b]*Shubnikov Institute of Crystallography, Russian Academy of Sciences, Moscow, 119333 Russia*
[c]*Tomsk Polytechnical University, Tomsk, 634050 Russia*

Submitted September 16, 2008

Abstract—The nature of luminescence bands prevailing in the near-edge spectrum of the CdS(O) crystals at high excitation intensities (10^{25}–10^{26} cm^{-3} s^{-1}) is clarified. It is shown that the alloys containing oxygen dissolved in II–VI crystals represent heterogeneous systems with oxygen segregating in the crystal matrix.

PACS numbers: 71.23.An, 71.55.Gs, 78.40.Fy, 78.55.Et, 78.66.Hf

DOI: 10.1134/S1063782609130028

In [1–6], a new approach is suggested to interpret the optical properties of II–VI crystals by the example of ZnS(O)–ZnSe(O) compounds containing the isoelectronic oxygen impurity. The interpretation is based on the conclusions of the theory of band anticrossing (BAC) [3, 4, 7, 8], which provides a means for taking into consideration the O_S atoms located at the lattice sites of the matrix. The BAC theory shows that the impurity of the isoelectronic oxygen acceptor interacting with the states of the conduction band induces splitting of the conduction band into the two subbands, the lower subband E_- and the upper subband E_+. In this study, using the same concept as a basis, we analyze some of the still unexplained specific features of luminescence of CdS near the fundamental absorption edge.

We studied single crystals grown on the oriented CdS crystals at the temperature 1100°C, and the pressure of vapor components was controlled during the growth. The procedure of growth was described elsewhere [9, 10]. The conditions of growth were varied within the region of existence of the compound, and the deviations from the stoichiometric composition were determined. The content of oxygen (as a background impurity) was estimated as the total content $[O]_{tot}$ by the procedure described in [11]. The content $[O]_{tot}$ was maximal (up to 2×10^{20}, sometimes 10^{21} cm^{-3}) in the samples with excess cadmium and, showing a stepwise change at the stoichiometric point, decreased to $\sim 10^{19}$ cm^{-3}, as the pressure of sulfur vapors in the growth region was increased [12, 13]. The shift of excitonic bands 10 (20) meV in the cathodoluminescence (CL) spectra studied with a broad beam at the energy 5–10 keV by the method of [10] did not represent any regular variations in the content of dissolved oxygen $[O_S]$ in the crystals under variations in their composition [13, 14].

Using a scanning electron microscope, we studied the microcathodoluminescence (MCL) spectra, the microstructure, and the microcomposition of the (0001) cuts of the grown crystals. The results show that the crystals are mosaic in structure, and the dimensions and the character of intergrowth of grains, the network of interfaces between the crystallites, and the character of irregularity inside the grains vary with deviations from the stoichiometric composition. It is reasonable to assume that, on cooling, oxygen forms segregates at defects in the material. The coarse (>150 μm) grains of CdS crystals with excess Cd decrease in size to 50–100 μm for nearly stoichiomentric compounds and to ~10 μm at maximal pressures of sulfur vapors. The typical feature of the samples is the layered compositional irregularity, with the layers parallel to the (0001) planes; such irregularity is more pronounced in the samples with excess cadmium. In the case of the maximal content of excess sulfur, some porosity is observed in the sample bulk.

The spatial distribution of defective regions in the samples becomes evident on etching. Some examples are shown in Fig. 1.

In order to exclude the effect of structural irregularities upon the results of studies of the optical properties of the CdS crystals in relation to their composition, we recorded the MCL spectra for individual single crystal grains. The MCL spectra were recorded with ×10000 magnification, most often for the 10 × 10 μm scanning area; the diameter of the beam was 1000 Å = 10^{-1} μm).

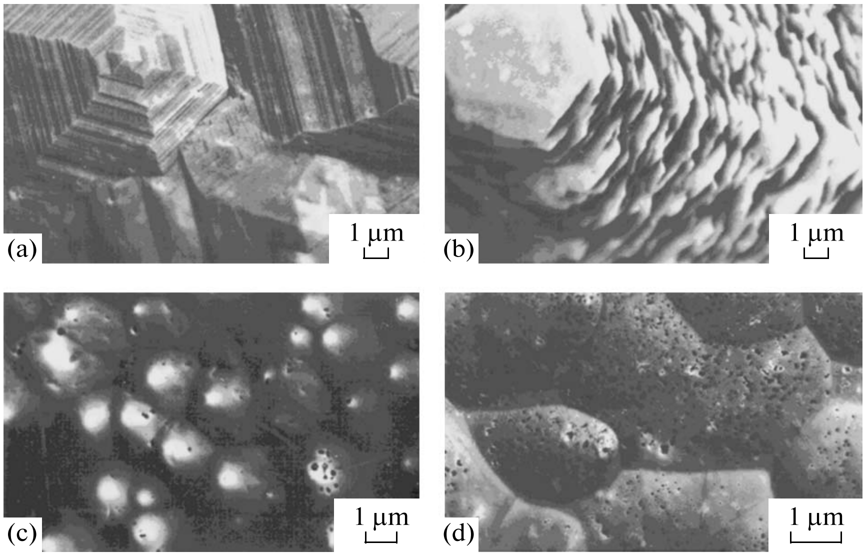

Fig. 1. SEM micrographs of the CdS(O) crystals: (a) coarse-grained CdS · Cd with a maximum excess pf oxygen; (b) the CdS · Cd grain after etching (the regions of removed layers in the (0001) planes are evident); (c) the CdS · S crystal with a maximum excess of sulfur; (d) the CdS · S grain after etching (multiple rounded pits are evident).

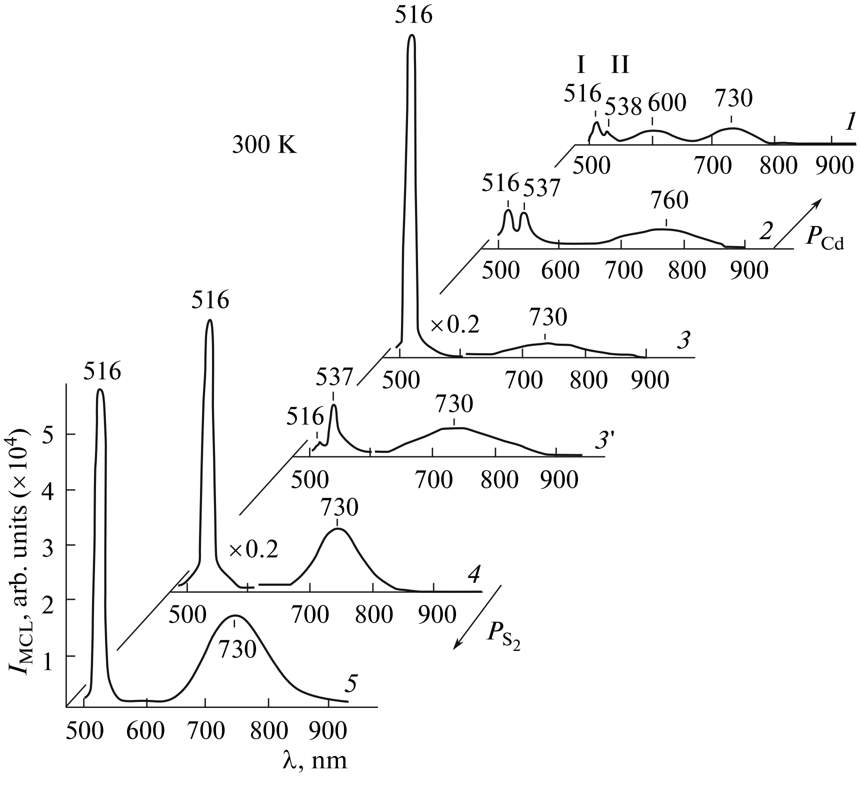

Fig. 2. MCL spectra recorded with the SEM microscope at the temperature 300 K, the energy of the electron beam 25 keV, and the excitation density $G = 10^{24}$ cm^{-3} s^{-1} for the compositionally different CdS(O) samples: (*3*, *3*') stoichiometric sample, (*2* ⟶ *1*) sample with excess cadmium, and (*4* ⟶ *5*) sample with excess sulfur. All of the spectra are recorded for the central part of individual single crystal grains, except curve *3*' obtained for the grain corner.

Temperature dependence of the spectral position of bands I and II in comparison with the position of the A_{ex} band in CdS

T, K	$\lambda(E)$						
	A_{ex}^{CdS}, nm (eV) **E_g, eV**	$A_{ex} - 1LO$, nm (eV)	I ($FE_{CdS \cdot O}$), nm (eV)	$A_{ex} - 2LO$, nm (eV)	$A_{ex} - 3LO$, nm (eV)	II (EE) ($LO = 0$, $[O] \longrightarrow 0$), nm (eV)	II (EE) ($LO = 0$, $[O] \neq 0$), nm (eV)
30	485.85 (2.5519) **2.5809**	493.14 (2.5142)	496 (2.4982)	500.6 (2.4765)	508.4 (2.4388)	505 (2.4535)	515.6 (2.4042)
77	487.17 (2.5450) **2.5740**	494.5 (2.5073)	498.9 (2.4853)	502.0 (2.4696)	509.8 (2.4319)	508 (2.4406)	518.5 (2.3913)
300	504.70 (2.4565) **2.4855**	512.6 (2.4188)	516 (2.4028)	520.7 (2.3811)	529.1 (2.3434)	526 (2.3571)	537 (2.3088)

Note: The positions of the bands at different temperatures T, K were calculated from the dependences $E(T) = E(0) - \gamma T^2/T + \delta$, where $\gamma = 9.7 \times 10^{-4}$ and $\delta = 600$ [18].

Figure 2 shows the evolution the MCL spectrum under variations in the composition of the samples produced at different excess pressures P_{S_2} and P_{Cd} of sulfur and cadmium vapors. From Fig. 2, we can see some regular trends dependent on the conditions of growth. However, in many cases, the MCL spectra recorded for different regions even of the same crystal are different. For example, curves *3* and *3'* refer to the same compositionally stoichiometric crystal.

The experimental data show that, in the region close to the fundamental absorption edge of CdS(O), the MCL spectra recorded at 300 K exhibit two bands of an unknown nature, one at 516 nm (band I) and the other at 537 nm (band II). At the same time, it is known that, at 300 K, the emission of free excitons A_{ex} corresponds to 504.7 nm and the green edge's emission of CdS is bound to be quenched with increasing temperature above 200 K [15, 14].

According to [16], the edge's emission bands (*EE*) shift with increasing temperature similar to how it happens with the excitonic spectra, and the activation energy of thermal quenching of the *EE* band is (0.14 ± 0.02) eV. It should be taken into consideration that, in the region of thermal quenching of the *EE* band, the orange band at ~640 nm intensifies.

To obtain more data, we recorded the pulsed cathodoluminescence (PCL) spectra and pulsed X-ray luminescence (PXRL) spectra, which provide information from deep within the crystal. Specifically, in the case of PCL at the average energy of the electron beam ~250 eV, the depth of the information layer is ~125 μm for CdS.

The procedure of measurements is described in [17]. We used two geometric layouts of experiments. In the case of layout 1, the sample was arranged at an angle of 45° to the direction of the electron beam, and the PCL or PXRL signal from the illuminated surface was detected. In the case of layout 2, we recorded the PCL signal from the cleaved facet in the direction orthogonal to the direction of incidence of the electron beam (at an angle of 90°).

The table lists the temperature-dependent positions of the basic emission bands in the region close to the optical absorption edge of CdS. This allows us to correlate the results obtained for MCL, PCL, etc., at different temperatures. Specifically, Figure 3 shows the PXRL and PCL spectra at the temperature 30 K for the stoichiometric CsS(O) sample.

Let us compare the spectra shown in Figs. 2 and 3a, taking into consideration the temperature shift of the emission bands in accordance with the change in the band gap of CdS $E_g(T)$ (see table). We can conclude that bands I (516 nm) and II (537 nm) evident in the MCL spectra at 300 K can be related to the bands observed at 30 K, first, to the 496 nm band unidentified so far and, second, to the leasing 515 nm line of the green edge's emission series typical of the CdS crystals.

The wavelength of bands I and II (see Fig. 2) is given from spectra of single crystal grains. Specifically, the most intense band, band I, is observed in the MCL spectra of different areas of crystals from 511 to 518 nm.

As can be seen from Fig. 3b, band I becomes observable, as the excitation density is increased. This fact was also mentioned previously; for example, in [14], it was shown that band I appeared, and then intensified almost linearly with increasing the SEM's excitation density and, at high excitation densities, band I prevailed in the spectrum. The appearance of emission

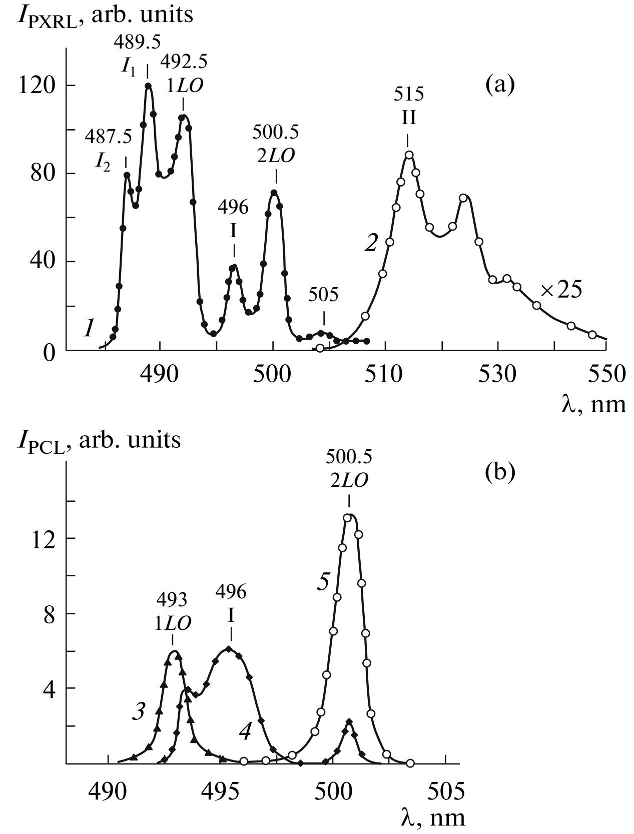

Fig. 3. (a) PXRL spectra of the compositionally stoichiometric CdS crystal, as recorded at 30 K (*1*) at the peak of the excitation pulse and (*2*) within 10 μs. (b) PCL spectra of the same CdS crystal at different excitation densities: $G = (3)\ 1.6 \times 10^{26}$, $(4)\ 4 \times 10^{26}$, and $(5)\ 6.5 \times 10^{26}$ $\text{cm}^{-3}\ \text{s}^{-1}$. The measurements were performed in geometric layout two at the peak of the excitation pulse. The bands denoted by I_1 and I_2 are typical of bound excitons in CdS.

band I at the excitation densities $\geq 10^{26}$ $\text{cm}^{-3}\ \text{s}^{-1}$ let the authors of [17] suggest that band I is due to recombination of charge carriers forming the electron–hole plasma.

However, band I is observable even at low excitation densities. Figure 4a exemplifies the CL spectra recorded with a broad beam at the excitation density $G \leq 10^{22}$ $\text{cm}^{-3}\ \text{s}^{-1}$ for the information layer less than 0.5 μm deep. For comparison, the spectra of the CdS · Cd sample kept in air for 7 months (Fig. 4a, curve *1*) and etched in HCl for 5 and 50 s are shown (Fig. 4a, curves *2*, *3*). It is evident that band I at 498 nm appears in the spectrum after disclosing the crystal bulk by etching.

After etching the crystal, there are also some changes in the edge emission. The edge emission of the unetched sample presents a band with a peak at 518 nm. However, after etching, the series of bands is always typical of the emission, with the LO motive and the leading line at shorter wavelengths, specifically, at 508 or 514 nm at 80 K (Fig. 4a).

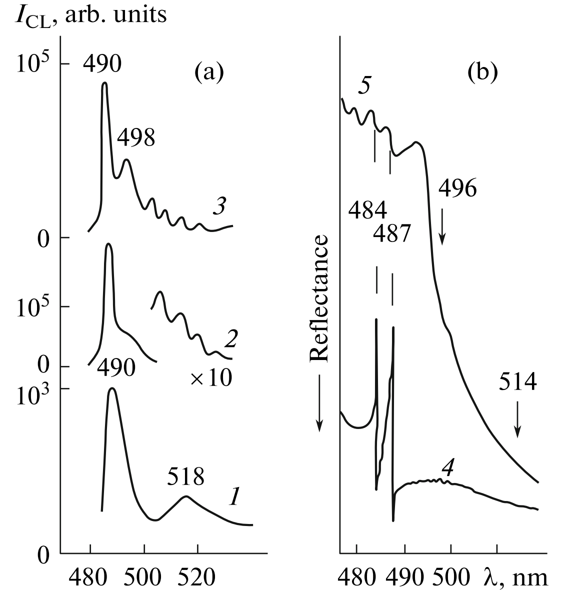

Fig. 4. (a) CL spectra recorded with a broad beam at the temperature 80 K (*1*) after ageing of the sample in air and (*2*, *3*) subsequent etching during (*2*) 5 and (*3*) 50 s. (b) Microphotograms of the reflectance spectra recorded at 77 K for CdS crystals with the concentration of oxygen (*4*) about 10^{19} and (*5*) 10^{20} cm^{-3}.

In studying the reflectance spectra of CdS in liquid nitrogen (see Fig. 4b), we also observe band I (the center of the band corresponds to ~496 nm). This band is particularly well pronounced for the layers doped with oxygen by ionic implantation [14]. In addition, in the reflectance spectra recorded at 77 K, we observe high extra absorption overlapping the excitonic spectral region of the matrix. At $[\text{O}]_{\text{tot}} < 10^{20}$ cm^{-3}, the extra absorption edge (EAE) is observed at 496–500 nm. If the concentration of oxygen is higher than 10^{20} (10^{21}) cm^{-3}, we observe also the second less-pronounced edge at 514–515 nm (Fig. 4b, curve *5*). The main EAE is bounded by reflectance band I. Band I has a shape typical of the exciton: exhibits a short-wavelength minimum of reflectance at 493–494 nm and a long-wavelength maximum at 498–500 nm.

Thus, band I can be observed also at low excitation intensities. This fact is inconsistent with the assumption that band I is related to the electron–hole plasma. Moreover, in [19], it was found that the I-type band of wurtzite was enhanced and shifted to longer wavelengths from the excitonic band A_{ex} with increasing excitation intensity, similar to what was observed in [17], but these effects were caused by the increase in the content of oxygen in the samples. It can be suggested that, in [17], such effects were due to the heterogeneity of the crystals under study. In addition, in [5, 6], the CL bands similar to band I were comprehensively described for ZnSe(O) and ZnS(O). The data reported in [5, 6] agree with the results obtained here for CdS and substantially supplement the data on band I under consideration. In ZnSe(O) and ZnS(O), bands I were observed only in crystals that exhibited self-activated (SA) emission; this gave grounds to relate bands I to excitons bound at SA centers. The excitonic nature and the unpredictability of such bands in the CL spectra at a small (~0.3 μm) depth of the information layer were confirmed, and it was found that these bands corresponded to emission from the sample bulk, being related to oxygen present in the matrix [3–6].

Reports on the anomalous long-wavelength excitonic band controlled by oxygen can be also found in publications [5, 20].

However, the interpretation of the nature of the bands as bands of bound excitons involves difficulties, specifically, because of the high binding energy of the exciton. For wurtzite with a high solubility of oxygen, the exciton's binding energy is even higher than 100 meV [2].

Supplementary data are obtained from the consideration of band II (see Fig. 2). It is not always possible to also interpret the nature of different series of the green edge's emission of CdS. In studying the specific features of edge emission in the pure CdS(O) crystals, whose composition differently deviated from stoichiometric relation, we obtained a number of results. At high excitation densities, the edge emission is clearly seen in the spectra of the crystals grown with excess cadmium and oxygen. Stabilization of the *EE* centers at the increased content of oxygen in crystals with excess cadmium was observed also in [14, 17]. According to the data obtained here, an increase in the pressure of sulfur vapors during the growth and a simultaneous decrease in the content of oxygen yield a decrease in the edge's emission intensity. Specifically, for the nearly stoichiometric CdS crystals, the edge emission is practically unobservable at the excitation density $G \sim 10^{25}$ cm^{-3} s^{-1}, whereas at the maximal excess of sulfur ("oxygen-free" CdS), only the low-intensity series with the leading line at 506 nm can be distinguished (at 47 K). This series was described previously in [10, 14, 21]. Taking into account the temperature shift (see table), we can conclude that the band at 506 nm corresponds to the leading lines of the same edge emission in CdS(O), if the depth of the acceptor level *EE* in these "oxygen-free" CdS crystals is assumed to be ~0.13 eV.

In the CdS(O) crystals, in different local areas, we observe different series of edge emission, with the leading lines corresponding to 508, 512, 515, 518 nm, etc., at 80 K., and the lines corresponding to longer wavelengths are observed for crystals containing more oxygen. In the context of the BAC theory, it can be suggested that, in the undoped special crystals with identical levels of impurity background, the different positions of the leading lines EE are defined by the same acceptor level, but these positions depend on variations in the band gap (the position of E_{-}) controlled by variations in the concentration of dissolved oxygen [O_S].

Estimation of possible changes in the band gap, $\Delta E_g(E_{-})$, under changes in the concentration of oxygen from the long-wavelength shift of the series *EE*, with the leading line at 515 nm typical of the crystals under consideration (see Fig. 3a), with respect to the 505 nm line observed for the "oxygen-free" CdS · S crystals at 30 K (see table) give ~50 (48) meV. It is found that band I observed at 516 nm in the excitonic MCL spectra at 300 K (Fig. 2) exhibits the same shift with respect to the *A* excitonic line in "oxygen-free" CdS. The extra absorption edge evident in the reflectance spectra and dependent on the concentration of oxygen [13, 14] is consistent with this shift of bands I and II as well [2–4].

Previously [1–6], it was established that the SA emission of ZnS and ZnSe was associated with oxygen segregates; in that case, the type-I bands were observed only in the crystals that exhibited the SA emission, i.e., contained oxygen segregates. The SA emission prevails at low excitation intensities ($\leq 10^{22}$ cm^{-3} s^{-1}); with elevating excitation level, the SA's emission intensity becomes saturated and, at the same time, excitonic band I increases in intensity [2, 3, 6, 12–14]. All these facts suggest that band I in the spectra CdS presents none other than free excitons of the CdS(O) alloy in oxygen segregates.

In contrast to the concept of excitons bound at SA centers, the conclusion that excitonic band I is associated with oxygen segregates provides an explanation to all contradictory observations. The elucidation of the role of oxygen segregates in the formation of the spectrum of CdS allows us to understand, among other things, why emission band I appears on excitation of the crystal bulk or at increased excitation intensities responsible for saturation of the SA luminescence and why band I shifts to longer wavelengths with increasing the concentration of oxygen.

The presence of oxygen segregates in the crystal bulk explains why the PCL spectra at 300 K do not correspond to the MCL spectra, especially when the PCL spectra are recorded after the excitation beam has propagated through the whole inhomogeneous sample (at an angle of 90° in layout 2). Such spectra recorded at high excitation intensities are exemplified in Fig. 5.

The origin of the broad bands shown in Fig. 5 is obviously complex. It is known that, as the excitation intensity is increased, the exciton–phonon interaction is enhanced and the *LO* phonon's replicas of the *A* excitonic band start to prevail in the spectra. The exciton–phonon interaction is considerably enhanced in the presence of isoelectronic impurities [22]. In addition, the broad band at 518–520 nm (Fig. 5a) can involve overlapping bands of different nature, first of all, the 2*LO* phonon replicas of the A_{ex} excitonic line of the matrix and excitonic band I of the CdS(O) segre-

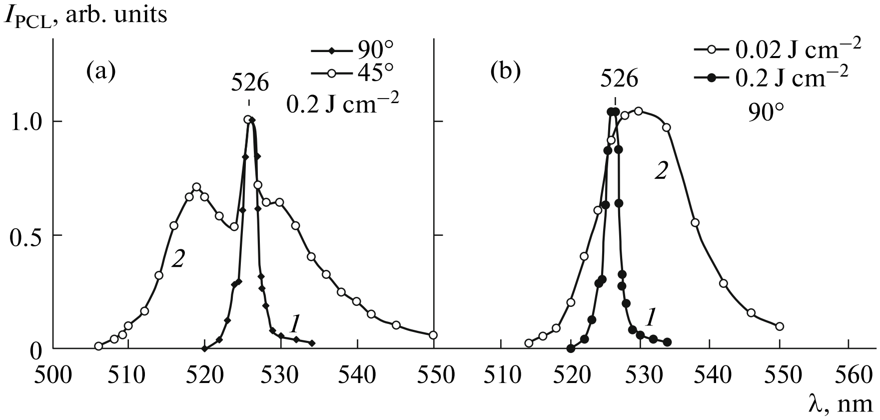

Fig. 5. PCL spectra recorded at 300 K for different regions of the CdS · Cd crystal with the nearly stoichiometric composition. The excitation density is $G = 10^{26}$ and 10^{27} cm^{-3} s^{-1} (corresponding to 0.02 and 0.2 J cm^{-2}, respectively). The beam emitted at the angles 90° and 45°.

gates in the bulk. The inhomogeneous broadening of these bands involving bands of compositionally different regions and segregates should be taken into consideration. The similar inference refers also to the broad band with a peak at about 530 nm spectrally corresponding to the 3*LO* replica of the A_{ex} line (Fig. 5b, curve *2*).

From the analysis of all available experimental data, it is possible to infer that the broadened spectrum (Fig. 5b, curve *2*) is typical of the crystals with excess cadmium and oxygen. The spectrum shown in Fig. 5a by curve *2* is characteristic of the crystals, in which the CdS(O) alloy decomposes to form the oxygen-free CdS regions [4–6]. The spectra of such type correspond also to the crystals grown at maximal pressures of sulfur vapors; in such crystals, there are grains free of oxygen. It is not improbable that the oxygen-free CdS regions are responsible for the narrow 526 nm band (see table). In [17], the 526 nm band is hypothetically attributed to stimulated emission at high excitation levels ($\geq 10^{26}$ cm^{-3} s^{-1}) and low temperatures (30 K), which is supported by a sharp increase in the emission intensity and by the appearance of directivity.

Thus, it is found that the crystals under consideration here present heterogeneous equilibrium systems stable in the bulk, in which oxygen segregates interact with the matrix during the formation of compositionally different regions as well as in the absorption–recombination processes. As shown in [4–6], oxygen segregates in the systems are responsible for many specific features of the optical properties of the crystals.

Since the electronegativity of the O_S centers is larger than the electronegativity of the host atoms of the matrix and the O_S centers attract electrons more strongly, the matrix serves as "an antenna" [22] that accumulates the excitation energy and transfers it to the isoelectronic impurity segregates. For the segregates, the bottom of the lower subband E_- is substantially below the bottom of the conduction band of the matrix, and this defines the high emission intensity in the region of such segregates. The complex multiband in the segregates is responsible for the SA emission bands at low excitation levels ($\leq 10^{22}$ cm^{-3} s^{-1}) or excitonic emission band I at high excitation levels (10^{25}–10^{26} cm^{-3} s^{-1}). In the oxygen segregates, wherein the concentration of oxygen [O_S] is higher, the edge emission is evident even at 300 K (Fig. 2).

According to the analysis, in this study, the oxygen concentration averaged over the volume in the CdS crystals, e.g., the compositionally stoichiometric crystals is about 10^{19} cm^{-3}. This concentration is consistent with the slight (no larger then 10–20 meV) shift of excitonic bands of the matrix. (The excitonic bands of the matrix are evident in the CL spectra recorded with a broad beam at a small depth of the information layer and in the reflectance spectra.) The experimentally observed shift of excitonic band I in the segregates can be as large as ~50 meV at the concentration of oxygen in the segregates about 10^{20} cm^{-3} [23].

As follows from the data of scanning electron microscopy (SEM), the segregates responsible for bands I are small (less than 0.1 μm) in size. Conglomerates of the segregates are two orders of magnitude larger. The conglomerates either have the shape of spherulites in the crystals with excess sulfur or form a layered structure with layers oriented in the (0001) plane, as established on etching of the samples (Fig. 1). Such systems can be formed as a result of coalescence on gas-static treatment [2, 3], cooling of the crystals with a sufficiently high initial concentration of dissolved oxygen [2–6], ion implantation of oxygen [2, 14], etc.

The conclusion that should be considered as being most important in the study is that the distribution of such isoelectronic impurity as oxygen that gives highly mismatched CdS(O), ZnS(O), and ZnSe(O) alloys is heterogeneous. In this case, in most crystals, the content of oxygen in the host's bulk matrix is much lower than the content in segregates.

The band model of the heterogeneous crystal's system containing oxygen segregates provides an adequate description of the absorption and emission of energy. Even if the matrix contains the SA's emission centers or exhibits the *EE* edge's emission, such radiation is emitted almost uniquely from the region of segregates. The segregates are responsible for the basic emission bands in the edge spectrum of the CdS(O) crystals studied here at 300 K. This is true also for the bands responsible for lasing [24]. The effect of lasing is of particular interest, since it suggests that the oxygen-containing crystal can serve as an efficient material for lasers.

Since the concentrations of oxygen in the segregates and in the matrix of CdS(O) can be different, the excitonic bands, SA emission, or *EE* edge's emission are variable in the spectral position.

REFERENCES

1. N. K. Morozova, I. A. Karetnikov, E. M. Gavrishchuk, et al., Fiz. Tekh. Poluprovodn. **38**, 39–43 (2004) [Sov. Phys. Semicond. **38**, 36 (2004)].
2. N. K. Morozova, I. A. Karetnikov, V. M. Lisitsyn, et al., Fiz. Tekh. Poluprovodn. **39**, 513–520 (2005) [Semiconductors **39**, 485 (2005)].
3. N. K. Morozova, D. A. Mideros, E. M. Gavrishuk, et al., Fiz. Tekh. Poluprovodn. **42**, 131–135 (2008) [Semiconductors **42**, 131 (2008)].
4. N. K. Morozova, D. A. Mideros, V. G. Galstyan, et al., Fiz. Tekh. Poluprovodn. **42**, 1039–1045 (2008) [Semiconductors **42**, 1023 (2008)].
5. N. K. Morozova, D. A. Mideros, Izv. Vyssh. Uchebn. Zaved., Ser. Élektron., No. 3, 3–10 (2008).
6. D. A. Mideros, Candidate's Dissertation in Mathematical Physics (Mosc. Énerg. Inst., Moscow, 2008).
7. W. Shan, W. Walukiewicz, J. W. Ager, et al., Phys. Rev. Lett. **82**, 1221–1224 (1999).
8. J. Wu, W. Walukiewicz, E. E. Haller, et al., Phys. Rev. B **65**, 2332101–2332104 (2002).
9. A. A. Davydov and E. B. Markov, Izv. AN SSSR, Ser. Neorg. Mater. **11**, 1755–1759 (1976).
10. A. V. Morozov, I. A. Karetnikov, V. L. Teplitskii, et al., Zh. Prikl. Spektrosk. **59**, 318–326 (1993).
11. V. S. Zimogorskii, N. A. Yashtulov, V. V. Blinov, et al., in *Proc. of the 30th Intern. Sci. Tech. Symp. on Noise and Degradation Processes in Semiconductor Devices, 29 Nov.–3 Dec. 1999, Moscow* (Mosc. Énerg. Inst., Moscow, 2000), pp. 211–215.
12. N. K. Morozova, A. V. Morozov, and B. C. Zimogorskii, Neorg. Mater. **29**, 1014–1019 (1993).
13. N. K. Morozova, A. V. Morozov, L. D. Nazarova, et al., Fiz. Tekh. Poluprovodn. **28**, 1699–1713 (1994) [Semiconductors **28**, 944 (1994)].
14. A. V. Morozov, Candidate's Dissertation in Mathematical Physics (Mosc. Énerg. Inst., Moscow, 1993).
15. N. A. Vlasenko, N. I. Vitrikhovskii, Z. L. Denisova, et al., Opt. Spektrosk. **21**, 466–475 (1966).
16. *Physics and Chemistry of A^2B^6 Compounds*, Ed. by S. A. Medvedev (Mir, Moscow, 1970) [in Russian].
17. V. I. Oleshko, S. S. Vil'chinskaya, V. I. Korepanov, et al., in *Proc. of the 6th Intern. Sci. Conf. on Radiation Thermal Effects and Processes in Inorganic Materials, 8–15 Aug. 2008, Tomsk* (Tomsk. Ped. Univ., Tomsk, 2008), pp. 922–927.
18. A. K. Dmitrienko, Fiz. Tekh. Poluprovodn. **19** (5), 20–27 (1985).
19. N. K. Morozova and M. M. Veselkova, Zh. Prikl. Spektrosk. **34**, 1094–1100 (1981).
20. A. Polimeni, M. Capizzi, Y. Nabetani, et al., Appl. Phys. Lett. **84**, 3304–3310 (2004).
21. C. G. van Doom, Solid State Commun. **3**, 355–356 (1965).
22. *Excitons*, Ed. by E. I. Rashba and M. D. Sturge (North-Holland, Amsterdam, 1982; Nauka, Moscow, 1965).
23. N. K. Morozova, V. I. Oleshko, N. D. Danilevich, et al., in *Proc. of the 39th Intern. Sci.-Tech. Symp. on Noise and Degradation processes in Semiconductor Devices, 25–28 Nov., 2008, Moscow* (Mosc. Énerg. Inst., Moscow, 2009), pp. 132–136.
24. I. M. Catalano, A. Cingoliani, and A. Minafra, Phys. Rev. B **8**, 1488–1492 (1973).